2019 13th European Conference on Antennas and Propagation (EUCAP)

Multi-Mode Antenna Concept based on Symmetry Analysis of Characteristic Modes

Authors:
Nikolai Peitzmeier
Dirk Manteuffel

Multi-Mode Antenna Concept based on Symmetry Analysis of Characteristic Modes

Nikolai Peitzmeier[1], Dirk Manteuffel[1],
[1]Institute of Microwave and Wireless Systems, Leibniz University Hannover, Hannover, Germany,
peitzmeier@hft.uni-hannover.de

***Abstract*—A multi-mode antenna concept based on a symmetry analysis of characteristic modes is presented for use in massive MIMO antenna arrays. A hexagonal plate is chosen as the basis of the antenna concept due to its interesting geometric properties. In particular, a symmetry analysis using group theory and representation theory is conducted in conjunction with a characteristic mode analysis, yielding that a hexagonal plate offers eight mutually orthogonal sets of characteristic surface current densities. On this basis, eight uncorrelated antenna ports are defined by means of the irreducible representations of the symmetry group.**

***Index Terms*—Group theory, characteristic modes, multiple-input multiple-output (MIMO), multi-mode antenna, symmetry.**

I. Introduction

The use of multi-mode antennas based on the theory of characteristic modes [1]–[3] has been presented in [4] to be a suitable approach for designing compact massive MIMO antenna arrays for future wireless communication systems. This is achieved by exciting different sets of characteristic modes on a single antenna element. Due to the orthogonality properties of the characteristic modes [2], the resulting antenna ports are uncorrelated. This way, multi-mode antenna elements with a compact form factor can be created, which may be arranged in an array in order to enable massive MIMO [4].

The conventional approach for designing multi-mode antennas using characteristic modes starts with a modal analysis of a given antenna. This analysis yields which modes are significant for radiation [5]. After suitable characteristic modes have been found, excitations are defined by inspecting the corresponding characteristic surface current densities. In recent designs, various excitation strategies are reported, e.g. inductive coupling elements (ICE), capacitive coupling elements (CCE) or slots [4], [6]–[8]. Furthermore, feeding (and matching) networks are often required as one antenna port may consist of several feed points on the antenna, which is usually attributed to symmetry properties of the characteristic surface current densities.

The above-mentioned exemplary multi-mode antenna designs offer up to four antenna ports. The simple question arises whether more antenna ports can be realized by making use of more significant characteristic modes, which would be beneficial for massive MIMO according to [9]. This question was examined in [10], where it was shown that, even though there is a large number of significant characteristic modes, only a limited number of uncorrelated antenna ports can be created due to the correlation of the characteristic surface current densities. It was further established that this correlation is related to the symmetry of the antenna.

Based on these findings, this paper aims at systematically exploiting the symmetry properties of characteristic modes in order to create uncorrelated antenna ports. For this purpose, an antenna geometry of high symmetry order, a hexagonal plate, is chosen based on a thorough symmetry analysis applying group theory and representation theory, which have already been used in conjunction with the theory of characteristic modes in [11]–[13] for other purposes. On this basis, it is shown that such a hexagonal geometry offers eight uncorrelated antenna ports. The hexagonal plate is therefore proposed as a starting point for the design of a multi-mode antenna which has up to eight uncorrelated antenna ports and may be arranged in a massive MIMO array (hexagonal tiling).

To this end, some important consequences of symmetry on the theory of characteristic modes are introduced in section II. After that, a symmetry analysis of the characteristic modes of a hexagonal plate is performed in section III. Based on this, an excitation is defined and analyzed in section IV. The results are summarized and discussed in section V.

II. Consequences of Symmetry on Characteristic Modes

The characteristic modes of an arbitrary perfectly electrically conducting (PEC) antenna are defined by the following generalized eigenvalue problem [2]:

$$X\left(\mathbf{J}_\nu\right) = \lambda_\nu R\left(\mathbf{J}_\nu\right), \tag{1}$$

where $\mathbf{J}_\nu$ denotes the ν-th characteristic surface current density (eigenfunction) of the antenna and λ_ν the corresponding eigenvalue. The linear operators R and X are the real and imaginary part, respectively, of the complex impedance operator Z derived from the electric field integral equation (EFIE) and the electric field boundary condition for perfect electric conductors.

The total surface current density on an antenna can be decomposed into a weighted sum of characteristic surface current densities [2]:

$$\mathbf{J} = \sum_\nu \alpha_\nu \mathbf{J}_\nu = \sum_\nu \frac{\left\langle \mathbf{J}_\nu, \mathbf{E}^i \right\rangle}{1 + j\lambda_\nu}\mathbf{J}_\nu = \sum_\nu \frac{\oiint_S \mathbf{J}_\nu \cdot \mathbf{E}^i \mathrm{d}S}{1 + j\lambda_\nu}\mathbf{J}_\nu, \tag{2}$$

where α_ν is called the modal weighting coefficient and its numerator is called the modal excitation coefficient. $\mathbf{E}^i$ denotes the incident electric field impressed e.g. by an antenna port. The integration is taken over the surface S of the antenna. The modal weighting coefficient describes how well an excitation couples to the ν-th characteristic surface current density and can be used to evaluate the effectiveness of a chosen excitation.

Although the characteristic surface current densities are orthogonal with respect to the impedance operator [2], they are in general not orthogonal to each other, which is expressed by the current correlation coefficient $\rho_{\mu\nu}$:

$$\rho_{\mu\nu} = \frac{\langle \mathbf{J}_\mu, \mathbf{J}_\nu \rangle}{\|\mathbf{J}_\mu\| \, \|\mathbf{J}_\nu\|} = \frac{\oiint_S \mathbf{J}_\mu \cdot \mathbf{J}_\nu \mathrm{d}S}{\sqrt{\oiint_S \mathbf{J}_\mu \cdot \mathbf{J}_\mu \mathrm{d}S}\sqrt{\oiint_S \mathbf{J}_\nu \cdot \mathbf{J}_\nu \mathrm{d}S}}. \quad (3)$$

This has the consequence that correlated characteristic surface current densities may not be excited separately, thus limiting the number of achievable antenna ports [10].

In [11], however, it is demonstrated that the characteristic surface current densities are basis functions of the irreducible representations of the symmetry group of an antenna. This is derived from the fact that the impedance operator in (1) is invariant under those geometric transformations which leave the antenna geometry invariant (symmetry operations). These symmetry operations form a mathematical group, which is called the symmetry group of the antenna [14].

The basis functions of the irreducible representations of the symmetry group have important orthogonality properties [14], which according to [11] apply to the characteristic surface current densities as follows:

$$\left\langle \mathbf{J}_m^{(p)}, \mathbf{J}_n^{(q)} \right\rangle = \oiint_S \mathbf{J}_m^{(p)} \cdot \mathbf{J}_n^{(q)} \mathrm{d}S = 0, \quad (4)$$

unless $p = q$ and $m = n$, where p and q denote different irreducible representations of the symmetry group and m and n different basis functions of a given representation. Equation (4) states that, first, characteristic surface current densities belonging to different representations are orthogonal to each other and, second, characteristic surface current densities forming a set of basis functions of the same multi-dimensional representation are orthogonal to each other. The number of mutually orthogonal sets of characteristic surface current densities can therefore be derived from the irreducible representations of the symmetry group of an antenna, which will be made use of in the following sections.

III. Symmetry Analysis of Hexagonal PEC Plate

In this section, an infinitely thin regular hexagonal PEC plate with an edge length of 0.7 wavelengths (0.7λ) as shown in Fig. 1 is analyzed. Its symmetry group is called D_6 (Schoenfliess notation) and it consists of the following twelve operations (with the Schoenfliess symbols in parentheses) [15]:

- the identity (E),
- the rotation by 60 ° about the z-axis (C_{6z}),
- the rotation by –60 ° about the z-axis (C_{6z}^{-1}),
- the rotation by 120 ° about the z-axis (C_{3z}),

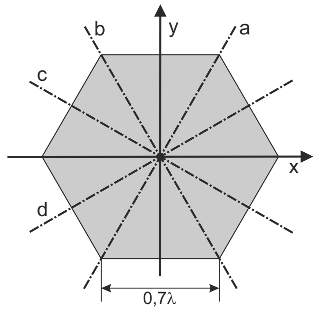

Fig. 1. Hexagonal plate and coordinate system.

- the rotation by –120 ° about the z-axis (C_{3z}^{-1}),
- the rotation by 180 ° about the z-axis (C_{2z}),
- the rotation by 180 ° about the x-axis (C_{2x}),
- the rotation by 180 ° about the y-axis (C_{2y}),
- the rotation by 180 ° about the diagonal a (C_{2a}),
- the rotation by 180 ° about the diagonal b (C_{2b}),
- the rotation by 180 ° about the diagonal c (C_{2c}),
- the rotation by 180 ° about the diagonal d (C_{2d}).

The symmetry group of the hexagonal plate has six irreducible representations $\Gamma^{(1)}$ to $\Gamma^{(6)}$ [15]. The representations map square matrices to the operations of the symmetry group which describe how the corresponding basis functions transform under the symmetry operations. The representation matrices are shown in Table I [14]. There are four one-dimensional representations $\Gamma^{(1)}$ to $\Gamma^{(4)}$ whose matrices are scalars. Accordingly, only one basis function belongs to each of these representations, which may be left either invariant (multplication with 1) or inverted (multiplication with –1) by the symmetry operations. Furthermore, there are two two-dimensional representations $\Gamma^{(5)}$ and $\Gamma^{(6)}$ with two-dimensional square matrices. A set of two basis functions belongs to each of these representations. A symmetry operation applied to one of these functions yields a linear combination of the two basis functions. Moreover, these two basis functions are degenerate, i.e. they have the same eigenvalue independent of frequency [11].

Now, the characteristic modes of the hexagonal PEC plate are calculated using an in-house method of moments software. A symmetric mesh is generated in order to reproduce the symmetry properties of the hexagonal plate. The edge length of the hexagon (0.7λ) has been chosen so that there are exactly eight significant characteristic modes (modal significance greater than $1/\sqrt{2}$) whose surface current densities all are different basis functions of the irreducible representations. The characteristic surface current densities of the significant modes are depicted in Fig. 2, with the principal current directions denoted by arrows. The modal significances are shown in Fig. 3, where some higher order modes are also taken into account.

By means of the current densities, each characteristic mode can now be assigned to one of the irreducible representations of the symmetry group of the hexagonal plate. This is done by applying the symmetry operations of the group to each current

TABLE I
REPRESENTATION MATRICES OF SYMMETRY GROUP D_6 OF HEXAGONAL PLATE

D_6	E	C_{2z}	C_{3z}	C_{3z}^{-1}	C_{6z}	C_{6z}^{-1}
$\Gamma^{(1)}$	1	1	1	1	1	1
$\Gamma^{(2)}$	1	1	1	1	1	1
$\Gamma^{(3)}$	1	-1	1	1	-1	-1
$\Gamma^{(4)}$	1	-1	1	1	-1	-1
$\Gamma^{(5)}$	$\begin{pmatrix} 1 & 0 \\ 0 & 1 \end{pmatrix}$	$\begin{pmatrix} -1 & 0 \\ 0 & -1 \end{pmatrix}$	$\begin{pmatrix} -1/2 & -\sqrt{3}/2 \\ \sqrt{3}/2 & -1/2 \end{pmatrix}$	$\begin{pmatrix} -1/2 & \sqrt{3}/2 \\ -\sqrt{3}/2 & -1/2 \end{pmatrix}$	$\begin{pmatrix} 1/2 & -\sqrt{3}/2 \\ \sqrt{3}/2 & 1/2 \end{pmatrix}$	$\begin{pmatrix} 1/2 & \sqrt{3}/2 \\ -\sqrt{3}/2 & 1/2 \end{pmatrix}$
$\Gamma^{(6)}$	$\begin{pmatrix} 1 & 0 \\ 0 & 1 \end{pmatrix}$	$\begin{pmatrix} 1 & 0 \\ 0 & 1 \end{pmatrix}$	$\begin{pmatrix} -1/2 & -\sqrt{3}/2 \\ \sqrt{3}/2 & -1/2 \end{pmatrix}$	$\begin{pmatrix} -1/2 & \sqrt{3}/2 \\ -\sqrt{3}/2 & -1/2 \end{pmatrix}$	$\begin{pmatrix} -1/2 & \sqrt{3}/2 \\ -\sqrt{3}/2 & -1/2 \end{pmatrix}$	$\begin{pmatrix} -1/2 & -\sqrt{3}/2 \\ \sqrt{3}/2 & -1/2 \end{pmatrix}$
D_6	C_{2x}	C_{2y}	C_{2a}	C_{2b}	C_{2c}	C_{2d}
$\Gamma^{(1)}$	1	1	1	1	1	1
$\Gamma^{(2)}$	-1	-1	-1	-1	-1	-1
$\Gamma^{(3)}$	1	-1	1	1	-1	-1
$\Gamma^{(4)}$	-1	1	-1	-1	1	1
$\Gamma^{(5)}$	$\begin{pmatrix} 1 & 0 \\ 0 & -1 \end{pmatrix}$	$\begin{pmatrix} -1 & 0 \\ 0 & 1 \end{pmatrix}$	$\begin{pmatrix} -1/2 & \sqrt{3}/2 \\ \sqrt{3}/2 & 1/2 \end{pmatrix}$	$\begin{pmatrix} -1/2 & -\sqrt{3}/2 \\ -\sqrt{3}/2 & 1/2 \end{pmatrix}$	$\begin{pmatrix} 1/2 & -\sqrt{3}/2 \\ -\sqrt{3}/2 & -1/2 \end{pmatrix}$	$\begin{pmatrix} 1/2 & \sqrt{3}/2 \\ \sqrt{3}/2 & -1/2 \end{pmatrix}$
$\Gamma^{(6)}$	$\begin{pmatrix} -1 & 0 \\ 0 & 1 \end{pmatrix}$	$\begin{pmatrix} -1 & 0 \\ 0 & 1 \end{pmatrix}$	$\begin{pmatrix} 1/2 & -\sqrt{3}/2 \\ -\sqrt{3}/2 & -1/2 \end{pmatrix}$	$\begin{pmatrix} 1/2 & \sqrt{3}/2 \\ \sqrt{3}/2 & -1/2 \end{pmatrix}$	$\begin{pmatrix} 1/2 & -\sqrt{3}/2 \\ -\sqrt{3}/2 & -1/2 \end{pmatrix}$	$\begin{pmatrix} 1/2 & \sqrt{3}/2 \\ \sqrt{3}/2 & -1/2 \end{pmatrix}$

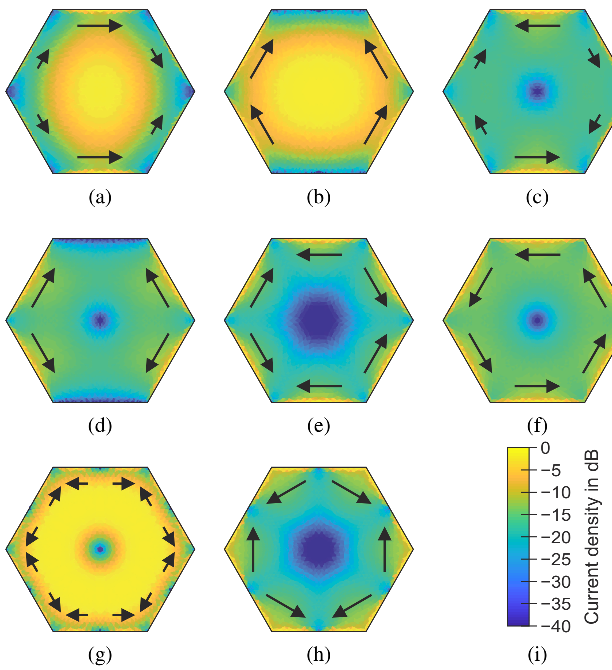

Fig. 2. Normalized surface current densities of significant characteristic modes of hexagonal PEC plate with principal current directions at the edges denoted by arrows. (a)-(h) Modes 1 to 8. (i) Colorbar.

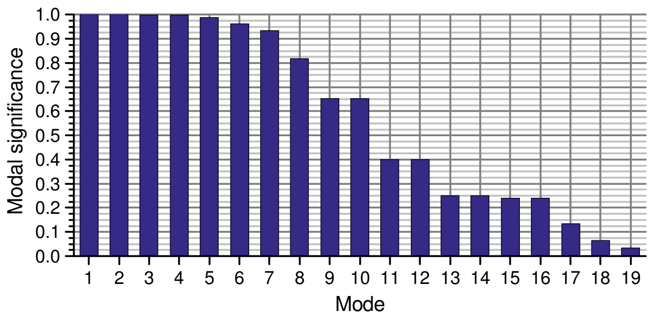

Fig. 3. Modal significances of hexagonal PEC plate.

TABLE II
ASSIGNMENT OF CHARACTERISTIC MODES OF HEXAGONAL PEC PLATE TO IRREDUCIBLE REPRESENTATIONS OF SYMMETRY GROUP D_6

Representation		Characteristic modes
$\Gamma^{(1)}$		7
$\Gamma^{(2)}$		6; 17
$\Gamma^{(3)}$		5; 19
$\Gamma^{(4)}$		8; 18
$\Gamma^{(5)}$	first	1; 9; 13
	second	2; 10; 14
$\Gamma^{(6)}$	first	3; 11; 15
	second	4; 12; 16

density and evaluating the transformed current densities. As an example, the surface current density of mode 7 (Fig. 2(g)) is invariant under all symmetry operations (multiplication with 1). This means that the corresponding representation matrices are all equal to one. Thus, the surface current density of mode 7 is a basis function of the first irreducible representation $\Gamma^{(1)}$. In the same way, those characteristic surface current densities forming a pair of basis functions of the two-dimensional representations can be identified. As an additional clue, the two basis functions must have the same eigenvalue, i.e. they are degenerate. For example, this is the case for modes 1 and 2 (Fig. 2(a) and (b)). They belong to the fifth representation $\Gamma^{(5)}$, which can be quickly checked

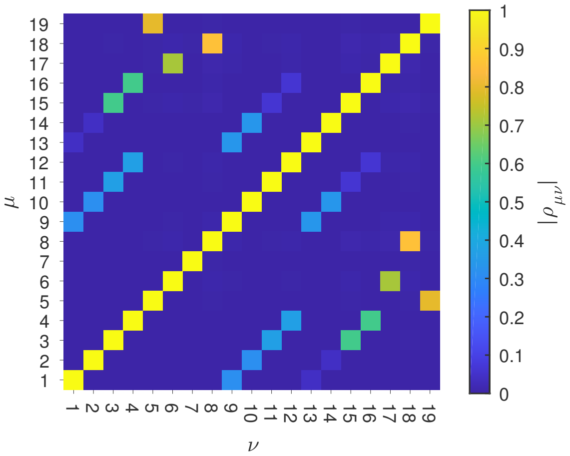

Fig. 4. Characteristic current correlation of hexagonal PEC plate.

by applying the rotation by 180° about the z-axis (C_{2z}), leaving the two current densities inverted (multiplication with the matrix $\left(\begin{smallmatrix}-1&0\\0&-1\end{smallmatrix}\right)$). By contrast, modes 3 and 4 (Fig. 2(c) and (d)), which are also degenerate, belong to the sixth representation $\Gamma^{(6)}$ which can be recognized by the fact that their current densities are invariant under the rotation by 180° about the z-axis (multiplication with the matrix $\left(\begin{smallmatrix}1&0\\0&1\end{smallmatrix}\right)$). The assignment of all characteristic modes to the irreducible representations of the symmetry group of the hexagonal plate is summarized in Table II.

The correlation of the characteristic surface current densities according to (3) is evaluated in Fig. 4. It is confirmed that characteristic surface current densities belonging to different irreducible representations and those forming a pair of basis functions of a two-dimensional representation are orthogonal to each other. Hence, the hexagonal plate offers eight mutually orthogonal sets of characteristic surface current densities, as expected.

IV. Excitation of Hexagonal PEC Plate based on Symmetry Analysis

The aim of this section is to make use of the orthogonality of the eight sets of characteristic modes verified in the previous section by defining eight uncorrelated antenna ports based on the symmetry of the hexagonal plate.

The modal excitation coefficient in (2) has the same form as the current correlation in (4). As a consequence, it is purposeful to define the antenna ports so that they behave like basis functions of the irreducible representations of the symmetry group, thus exploiting the orthogonality properties. To this end, the antenna ports need to consist of several feed points which are driven simultaneously in such a way that they transform according to Table I.

One solution, which uses only feed points at the edges of the plate, is shown in Fig. 5. It may be derived manually or by using automated procedures (projection operators [14]). It is optimal in the sense that it consists of as few feed points as possible while fulfilling the symmetry requirements of the different representations.

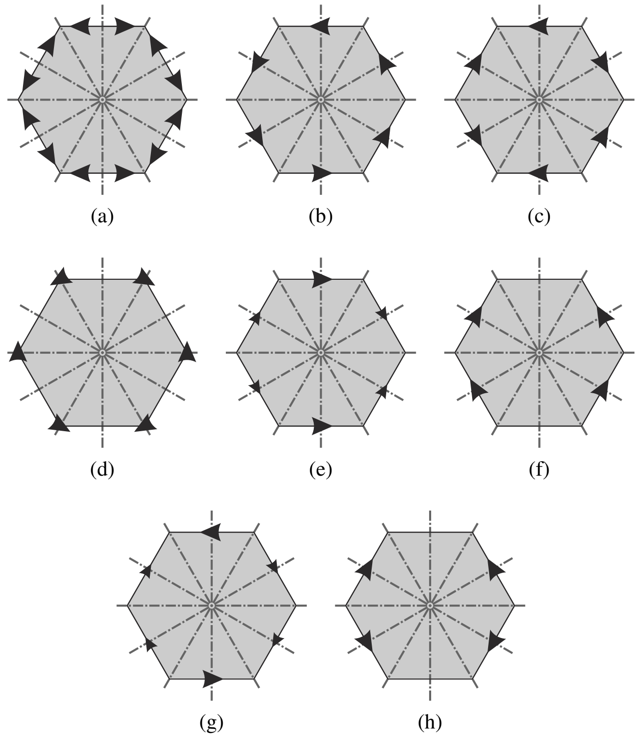

Port	1	2	3	4	5	6	7	8
Repr.	$\Gamma^{(1)}$	$\Gamma^{(2)}$	$\Gamma^{(3)}$	$\Gamma^{(4)}$	$\Gamma^{(5)}_1$	$\Gamma^{(5)}_2$	$\Gamma^{(6)}_1$	$\Gamma^{(6)}_2$
Fig.	5(a)	5(b)	5(c)	5(d)	5(e)	5(f)	5(g)	5(h)

(i)

Fig. 5. Port definition of hexagonal PEC plate. The small arrows denote half the feed voltage of the large arrows. (a)-(h) Ports 1 to 8. (i) Assignment to irreducible representations.

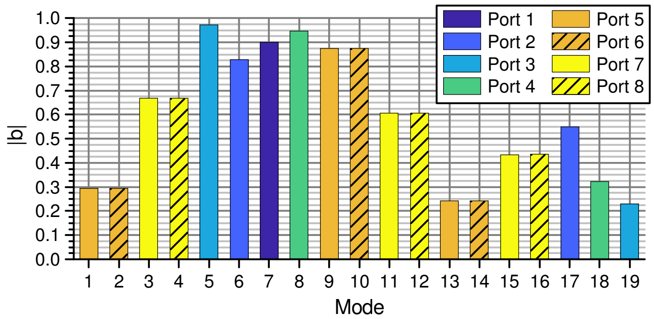

Fig. 6. Absolute values of normalized modal weighting coefficients b of hexagonal PEC plate excited according to Fig. 5.

In order to evaluate the excitation, the feed points are represented by small voltage gap sources in the method of moments [16] and the normalized modal weighting coefficients as defined in [17] are examined in Fig. 6. It is clearly visible that the sets of characteristic modes excited by the antenna ports are exactly those sets defined by the irreducible representations of the symmetry group listed in Table II, as intended. It is noteworthy that some higher order modes also have

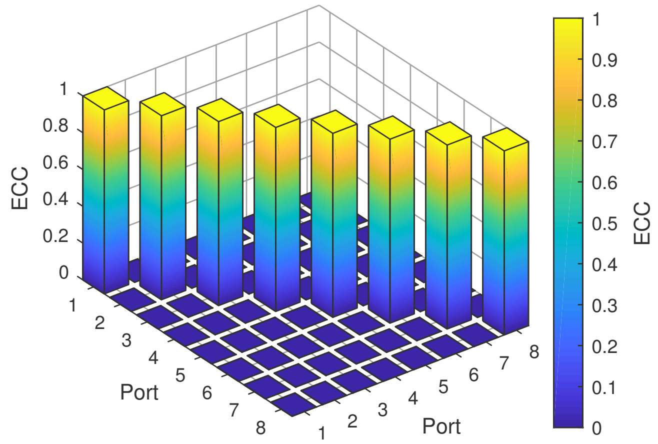

Fig. 7. Envelope correlation coefficients (ECC) of hexagonal PEC plate excited according to Fig. 5.

comparatively high weighting coefficients which may have an impact on the input impedance of the ports. Nevertheless, as mutually orthogonal sets of characteristic modes are excited, the antenna ports are uncorrelated, which is confirmed by the envelope correlation coefficients (ECC) in Fig. 7 calculated from the total radiated far fields [17].

It should be noted that this result is also valid if the idealized sources used in the previous simulations are replaced by practical excitation elements as long as the symmetry of the resulting antenna geometry is maintained, i.e. the symmetry group is still D_6. This can for example be achieved by using symmetric inductive coupling elements (cf. [6]) or slots (cf. [4]) at the feed points in Fig. 5.

V. Conclusion

A multi-mode antenna concept based on a hexagonal plate is presented which is intended for use as an element of a massive MIMO array. The antenna concept is developed by systematically exploiting the symmetry properties of a regular hexagon. By means of group theory and representation theory, it is shown that there are eight mutually orthogonal sets of characteristic modes. On this basis, eight uncorrelated antenna ports are realized by inspecting the matrix representations.

The antenna ports and feed points defined in this work can be used as a starting point for the next design steps, which comprise implementing suitable excitation elements like ICE or CCE and the design of a feed network as well as impedance matching. As already discussed in section IV, the antenna ports remain uncorrelated as long as the symmetry of the complete antenna is maintained. It will be the focus of upcoming research how well this criterion can be fulfilled throughout the design process and what impact the excitation elements, the feed network and other practical constraints have. The final aim of this research campaign is the design of a complete prototype based on the promising results of this work.

Acknowledgment

This work was funded by Deutsche Forschungsgemeinschaft (DFG) within the priority program SPP 1655 under grant MA 4981/4-2.

References

[1] R. Garbacz and R. Turpin, "A generalized expansion for radiated and scattered fields," *IEEE Transactions on Antennas and Propagation*, vol. 19, no. 3, pp. 348–358, May 1971.

[2] R. Harrington and J. Mautz, "Theory of characteristic modes for conducting bodies," *IEEE Transactions on Antennas and Propagation*, vol. 19, no. 5, pp. 622–628, Sep 1971.

[3] ——, "Computation of characteristic modes for conducting bodies," *IEEE Transactions on Antennas and Propagation*, vol. 19, no. 5, pp. 629–639, Sep 1971.

[4] D. Manteuffel and R. Martens, "Compact multimode multielement antenna for indoor UWB massive MIMO," *IEEE Transactions on Antennas and Propagation*, vol. 64, no. 7, pp. 2689–2697, July 2016.

[5] M. Cabedo-Fabres, E. Antonino-Daviu, A. Valero-Nogueira, and M. Bataller, "The theory of characteristic modes revisited: A contribution to the design of antennas for modern applications," *Antennas and Propagation Magazine, IEEE*, vol. 49, no. 5, pp. 52–68, Oct 2007.

[6] R. Martens and D. Manteuffel, "Systematic design method of a mobile multiple antenna system using the theory of characteristic modes," *IET Microwaves, Antennas Propagation*, vol. 8, no. 12, pp. 887–893, Sept 2014.

[7] M. Bouezzeddine and W. L. Schroeder, "Design of a wideband, tunable four-port MIMO antenna system with high isolation based on the theory of characteristic modes," *IEEE Transactions on Antennas and Propagation*, vol. 64, no. 7, pp. 2679–2688, July 2016.

[8] D. W. Kim and S. Nam, "Systematic design of a multiport MIMO antenna with bilateral symmetry based on characteristic mode analysis," *IEEE Transactions on Antennas and Propagation*, vol. 66, no. 3, pp. 1076–1085, March 2018.

[9] N. Doose and P. A. Hoeher, "Massive MIMO ultra-wideband communications using multi-mode antennas," in *SCC 2015; 10th International ITG Conference on Systems, Communications and Coding*, Feb 2015, pp. 1–6.

[10] N. Peitzmeier and D. Manteuffel, "Selective excitation of characteristic modes on an electrically large antenna for MIMO applications," in *2018 12th European Conference on Antennas and Propagation (EUCAP)*, April 2018.

[11] J. Knorr, "Consequences of symmetry in the computation of characteristic modes for conducting bodies," *IEEE Transactions on Antennas and Propagation*, vol. 21, no. 6, pp. 899–902, Nov 1973.

[12] K. R. Schab and J. T. Bernhard, "A group theory rule for predicting eigenvalue crossings in characteristic mode analyses," *IEEE Antennas and Wireless Propagation Letters*, vol. 16, pp. 944–947, 2017.

[13] M. Masek, M. Capek, and L. Jelinek, "Modal tracking based on group theory," in *2018 12th European Conference on Antennas and Propagation (EUCAP)*, April 2018.

[14] J. F. Cornwell, *Group Theory in Physics: An Introduction*. San Diego, CA, USA: Academic Press, 1997.

[15] G. F. Koster, *Properties of the Thirty-Two Point Groups*. Cambridge, MA, USA: M.I.T. Press, 1963.

[16] S. N. Makarov, *Antenna and EM Modeling with MATLAB*. New York, NY, USA: Wiley, 2002, pp. 60–62.

[17] E. Safin and D. Manteuffel, "Reconstruction of the characteristic modes on an antenna based on the radiated far field," *IEEE Transactions on Antennas and Propagation*, vol. 61, no. 6, pp. 2964–2971, June 2013.